On metric structure of ultrametric spaces

2004 J. Phys. A: Math. Gen. 37 3783

(http://iopscience.iop.org/0305-4470/37/12/005)

INSTITUTE OF PHYSICS PUBLISHING JOURNAL OF PHYSICS A: MATHEMATICAL AND GENERAL

J. Phys. A: Math. Gen. **37** (2004) 3783–3803 PII: S0305-4470(04)70237-1

On metric structure of ultrametric spaces

S K Nechaev[1,2] **and O A Vasilyev**[2]

[1] LPTMS, Université Paris Sud, 91405 Orsay Cedex, France
[2] Landau Institute for Theoretical Physics, 117334, Moscow, Russia

Received 12 October 2003, in final form 20 January 2004
Published 10 March 2004
Online at stacks.iop.org/JPhysA/37/3783 (DOI: 10.1088/0305-4470/37/12/005)

Abstract
In our work we have reconsidered the old problem of diffusion at the boundary of an ultrametric tree from a 'number theoretic' point of view. Namely, we use the modular functions (in particular, the Dedekind η-function) to construct the 'continuous' analogue of the Cayley tree isometrically embedded in the Poincaré upper half-plane. Later we work with this continuous Cayley tree as with a standard function of a complex variable. In the framework of our approach, the results of Ogielsky and Stein on dynamics in ultrametric spaces are reproduced semi-analytically or semi-numerically. The speculation on the new 'geometrical' interpretation of replica $n \to 0$ limit is proposed.

PACS numbers: 64.70.Pf, 02.70.Uu, 02.40.Tt

1. Introduction

Let us begin with an obvious and almost tautological statement: any regular tree has an ultrametric structure. Recall that ultrametricity of the space $\mathcal{H}$ implies the 'strong triangle inequality' meaning that the distances r_{AB}, r_{BC} and r_{AC} between any three points A, B, C in the space $\mathcal{H}$ satisfy the condition $r_{AC} \leqslant \max\{r_{AB}, r_{BC}\}$ (see, for example, [1]). Appearing in the mathematical literature in connection with p-adic analysis (see, for a review, [2, 3]), ultrametric spaces became very popular with the physical community because of their importance for spin glasses (see, for a review, [4], and references therein).

The famous replica symmetry breaking (RSB) scheme [5] is ultimately connected to the ultrametric structure of the phase space of many disordered systems possessing spin-glass behaviour. Since the invention of RSB, many authors, both physicists and mathematicians, have attempted to adapt the p-adic analysis for physical needs mainly trying to elucidate and justify the replica $n \to 0$ limit. However, from our point of view, the interpretation of spin-glass problems in terms of p-adic language does not converge well. As an exception one has to mention recent interesting contributions to that subject [6–8], where the application of p-adic Fourier transform allows us to significantly simplify the solution to the problem of diffusion on the ultrametric tree. One can hope that the continuation and generalization of these works would lead to deeper penetration of p-adic analysis into physics of disordered systems with

ultrametric phase spaces, such as spin glasses, neural networks and disordered heteropolymers (see [8, 9] for a detailed list of corresponding references).

In what follows we shall always keep in mind the $(p+1)$-branching Cayley tree as an example of an ultrametric space. Despite the extremely simple topological structure of a tree, one cannot operate in this space as in the usual space with a Euclidean metric because the number of degrees of freedom for the $(p+1)$-branching Cayley tree increases exponentially with the size of the tree. For some problems, such as, for example, the branching process on Cayley trees and tree-like graphs, it is not sufficient to deal only with the 'distance' measured in number of generations between two points on the graph, but it is ultimately necessary to know the absolute values of coordinates of points on the Cayley tree. The main difficulty concerns the encoding of the Cayley tree vertices. This problem becomes very cumbersome because for the tree we do not have any transparent and convenient 'coordinate system', such as a D-dimensional grid in a D-dimensional Euclidean space. One of the possible ways to resolve the addressed problem consists in using p-adic analysis [10, 11]. The vertices of the graph $\mathcal{C}$, i.e. of the $(p+1)$-branching Cayley tree, admit the natural parametrizations by the p-adic numbers which enables us to develop the whole machinery like the p-adic Fourier transform etc. This method has been exploited in [6–8].

Another possibility that is described in this paper consists in the following. Instead of working with the ultrametric discrete graph $\mathcal{C}$, one can embed this graph in the metric space $\mathcal{H}$ preserving all ultrametric properties of $\mathcal{C}$. Let us mention that any image of a regular Cayley tree refers indirectly to the isometric embedding of a tree into the complex plane. Indeed, the Cayley tree is usually drawn in the picture in such a way that any new generation of vertices (counted from the root point) is smaller than the previous generation in geometric progression. Taking advantage of the isometric embedding, one can

- naturally parametrize the vertices of the Cayley graph $\mathcal{C}$ by an ordinary complex variable $z = x + \mathrm{i}y$ in the complex plane z without using any ingredients of a p-adic analysis;
- construct a continuous analogue of a Cayley tree, i.e. a continuous space $\mathcal{H}$ with ultrametric properties borrowed from the initial Cayley tree.

The paper is organized as follows. In section 2 we describe the method of isometric embedding of the regular 3-branching Cayley tree $\mathcal{C}$ into the complex upper half-plane $z = x + \mathrm{i}y$, also we discuss the ultrametric properties of the resulting space $\mathcal{H}$. The problem of diffusion on the boundary of ultrametric tree $\mathcal{C}$ embedded into the space $\mathcal{H}$ is considered in section 3. The results are summarized in the conclusion, where we express some conjectures concerning the possible geometrical interpretation of replica $n \to 0$ limit.

2. Ultrametric structure of isometric Cayley trees

It is well known that any regular Cayley tree, as an exponentially growing structure, cannot be isometrically embedded in a Euclidean plane. Recall that the embedding of a Cayley tree $\mathcal{C}$ into the metric space is called 'isometric' if $\mathcal{C}$ covers that space, preserving all angles and distances. For example, the rectangular lattice isometrically covers the Euclidean plane $\mathcal{E} = \{x, y\}$ with the flat metric $\mathrm{d}s^2 = \mathrm{d}x^2 + \mathrm{d}y^2$. In the same way the Cayley tree $\mathcal{C}$ isometrically covers the surface of constant negative curvature (the Lobachevsky plane) $\mathcal{H}$. One of the possible representations of $\mathcal{H}$, known as a Poincaré model, is the upper half-plane $\mathrm{Im}\, z > 0$ of the complex plane $z = x + \mathrm{i}y$ endowed with the metric $\mathrm{d}s^2 = \frac{\mathrm{d}x^2 + \mathrm{d}y^2}{y^2}$ of constant negative curvature. In this section we aim to construct the 'continuous' analogue of the standard 3-branching Cayley tree by means of modular functions and analyse the structure of the

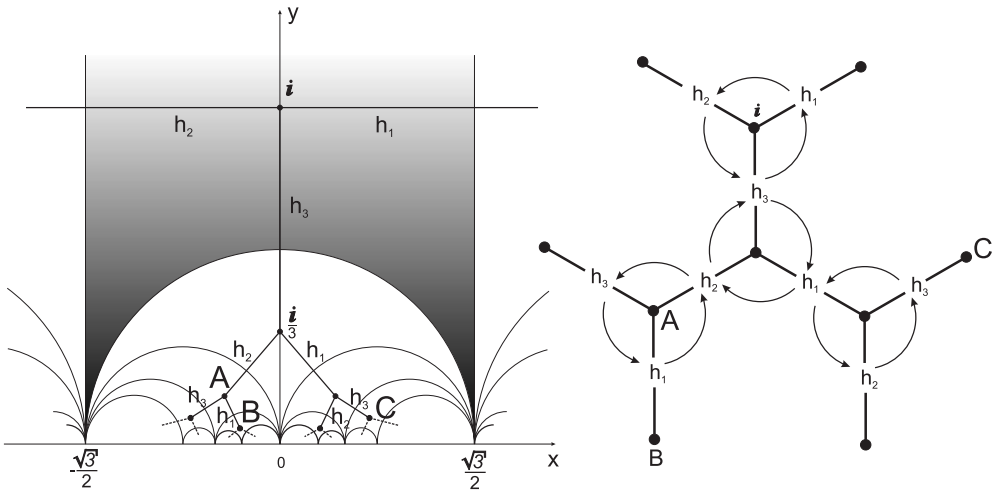

Figure 1. Left: schematic construction of the Cayley tree in the upper half-plane $y = \mathrm{Im}\, z > 0$. Right: periodic orientation of generators corresponding to neighbouring branches (shown by arrows).

barriers separating the neighbouring valleys. Due to specific number-theoretic properties of modular functions these barriers are ultrametrically organized.

2.1. Continuous analogue of isometric Cayley tree

To be precise, let us begin with the explicit description of the standard recursive construction which allows encoding of all vertices of the 3-branching Cayley tree $\mathcal{C}$ isometrically covering the surface of the constant negative curvature $\mathcal{H} = \{z|\mathrm{Im}\, z > 0\}$. Recall that the 3-branching Cayley tree is the Cayley graph of the group Λ having the free product structure: $\Lambda \sim \mathbb{Z}_2 \otimes \mathbb{Z}_2 \otimes \mathbb{Z}_2$ (where $\mathbb{Z}_2$ is the cyclic group of second order). The matrix representation of the generators h_1, h_2, h_3 of the group Λ is well known (see, for example, [12]):

$$h_1 = \begin{pmatrix} 1 & -\frac{2}{\sqrt{3}} \\ 0 & -1 \end{pmatrix} \qquad h_2 = \begin{pmatrix} 1 & \frac{2}{\sqrt{3}} \\ 0 & -1 \end{pmatrix} \qquad h_3 = \begin{pmatrix} 0 & \frac{1}{\sqrt{3}} \\ \sqrt{3} & 0 \end{pmatrix}. \tag{1}$$

The Cayley tree isometrically embedded in $\mathcal{H}$ can be recursively constructed. This construction is illustrated in figure 1. Specifically, we proceed as follows. Take a point $z_0 = \mathrm{i}$, which is the centre of the shaded domain. This point is the origin of the forthcoming Cayley tree. Then we find a point symmetric with the point z_0 with respect to one of the boundaries of the shaded *circular triangle* (namely, the semicircle touching the boundary $y = 0$ at the points $-\frac{\sqrt{3}}{2}$ and $\frac{\sqrt{3}}{2}$). This way we get a point $z_1 = \frac{\mathrm{i}}{3}$. The point A is the point symmetric with z_1 with respect to the semicircle touching the boundary $y = 0$ at the points $-\frac{\sqrt{3}}{2}$ and 0.

The general prescription to find the coordinates of all vertices of the Cayley tree $\mathcal{C}$ in $\mathcal{H}$ is as follows: (i) choose the point $z_0 = \mathrm{i}$ as the root of the tree; (ii) take generators h_1, h_2, h_3 (see equation (1)) and attribute them with the branches of the Cayley tree according to the rule: one generator corresponds to one branch and any vertex of the tree connects three branches associated with three *different* generators h_1, h_2, h_3; (iii) define the cyclic orientation of the generators on the tree: the root $z_0 = \mathrm{i}$ connects h_1, h_2, h_3 with counterclockwise orientation. Any two nearest neighbouring vertices have opposite orientation of h_1, h_2, h_3 (see figure 1);

(iv) associate any vertex in the generation n from the root point of the tree $\mathcal{C}$ with an element M_n of the group Λ (where $\alpha_k \in \{1, 2, 3\}$ for any k):

$$M_n = \begin{pmatrix} a & b \\ c & d \end{pmatrix} = \prod_{k=1}^{n} h_{\alpha_k}.$$

The coordinates of the Cayley tree vertices are obtained by the right-hand side multiplication of the 2×2 matrices h_i from the root $z_0 = \mathrm{i}$ to the point of destination, z_{fin}. The explicit construction depends on the number of steps n to the root point and is different for even and odd n:

$$\begin{cases} z_{\mathrm{fin}} = \dfrac{a\bar{z}_0 + b}{c\bar{z}_0 + d} & \text{for} \quad \text{odd } n \\ z_{\mathrm{fin}} = \dfrac{az_0 + b}{cz_0 + d} & \text{for} \quad \text{even } n. \end{cases} \tag{2}$$

For example, the coordinates of the points z_A, z_B, z_C in figure 1 are

$$M_2^A = h_3h_2 = \begin{pmatrix} 0 & -\frac{1}{\sqrt{3}} \\ \sqrt{3} & 2 \end{pmatrix} \qquad z_A = -\frac{2}{7\sqrt{3}} + \frac{\mathrm{i}}{7}$$

$$M_3^B = h_3h_2h_3 = \begin{pmatrix} -1 & 0 \\ 2\sqrt{3} & 1 \end{pmatrix} \qquad z_B = -\frac{4}{19\sqrt{3}} + \frac{\mathrm{i}}{19}$$

$$M_3^C = h_3h_1h_2 = \begin{pmatrix} 0 & \frac{1}{\sqrt{3}} \\ \sqrt{3} & 4 \end{pmatrix} \qquad z_C = \frac{2\sqrt{3}}{13} + \frac{\mathrm{i}}{13}.$$

To establish the relation with the forthcoming constructions, we shall make the simple linear transform of $z : z \to \frac{\sqrt{3}}{2}z + \frac{1}{2}$. The coordinates of the points A and B are shown in figure 2 after such transform.

However, such recursive construction has, from our point of view, a crucial shortcoming: one cannot automatically encode all vertices of the tree introducing a sort of a 'coordinate system' as, say, in the Euclidean plane. Actually, we know that any vertex of a rectangular grid in the Euclidean plane has the coordinates (am, bn), where $\{m, n\} \in Z$ and (a, b) are the length and the width of the elementary cell of the lattice. Our desire is to construct something similar for homogeneous trees. To be more specific, we aim to find an analytic function $f(z)$ defined in $\mathrm{Im}\, z > 0$ all of whose zeros give all coordinates of the vertices of the 3-branching homogeneous Cayley tree $\mathcal{C}$ isometrically embedded into $\mathcal{H}(z|\mathrm{Im}\, z > 0)$. In rest of this section we describe the construction of the corresponding function $f(z|\mathrm{Im}\, z > 0)$ and discuss its properties in connection with the geometry of ultrametric spaces. The forthcoming construction is based on the properties of the Dedekind η-function. Recall the standard definition of the $\eta(z)$-function (see, for instance, [13]):

$$\eta(z) = \mathrm{e}^{\pi \mathrm{i} z/12} \prod_{k=0}^{\infty} (1 - \mathrm{e}^{2\pi \mathrm{i} k z}) \qquad \mathrm{Im}\, z > 0. \tag{3}$$

It is well known [13] that the Dedekind η-function is connected to the elliptic Jacobi ϑ-functions by the following relation:

$$\vartheta_1'(0, \mathrm{e}^{\pi \mathrm{i} z}) = \eta^3(z) \tag{4}$$

where

$$\vartheta_1'(0, \mathrm{e}^{\pi \mathrm{i} z}) \equiv \left. \frac{\mathrm{d}\vartheta_1(u, \mathrm{e}^{\pi \mathrm{i} z})}{\mathrm{d}u} \right|_{u=0} = 2\, \mathrm{e}^{\pi \mathrm{i} z/4} \sum_{n=0}^{\infty} (-1)^n (2n+1)\, \mathrm{e}^{\pi \mathrm{i} n(n+1) z}. \tag{5}$$

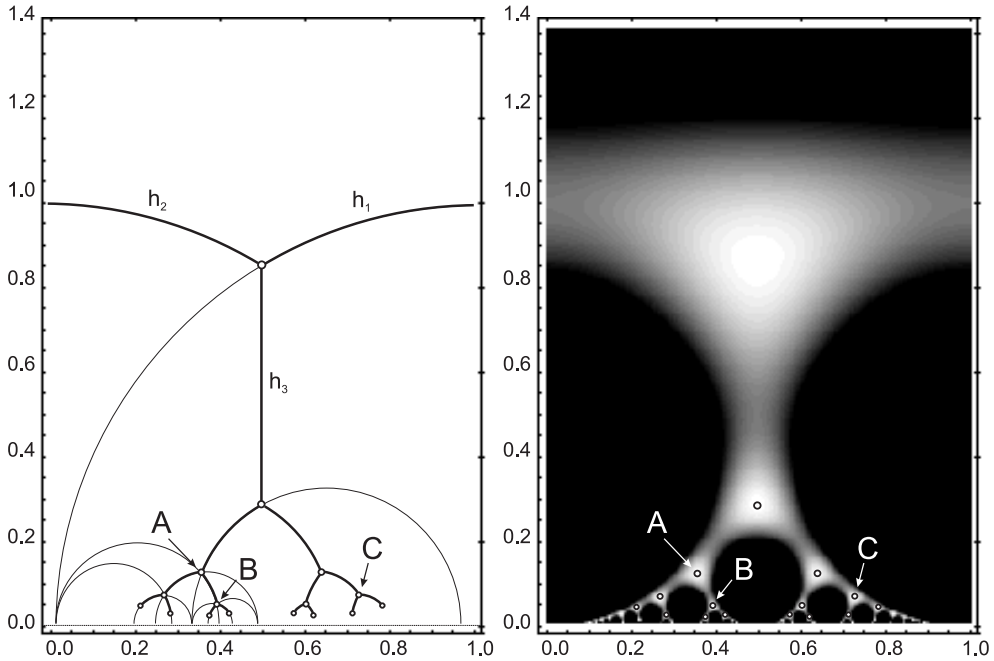

Figure 2. Left: 3-branching Cayley tree isometrically embedded in Poincaré hyperbolic upper half-plane $\mathcal{H}$. Right: density plot of the function $f(z)$ (see text) in the rectangle $\{0 \leqslant \mathrm{Re}\, z \leqslant 1, 0.01 \leqslant \mathrm{Im}\, z \leqslant 1.4\}$.

Now we are in a position to formulate the central assertion of the paper. Define the function $f(z)$ as follows:

$$f(z) = C^{-1}|\eta(z)|(\mathrm{Im}\, z)^{1/4} \tag{6}$$

where C is the normalization constant,

$$C = \left|\eta\left(\frac{1}{2} + \mathrm{i}\frac{\sqrt{3}}{2}\right)\right| \left(\frac{\sqrt{3}}{2}\right)^{1/4} = 0.772\,301\,84\ldots. \tag{7}$$

The normalization constant C is chosen to set the maximal value of the function $f(z)$ to 1: $0 < f(z) \leqslant 1$ for any z in the upper half-plane $\mathrm{Im}\, z > 0$. It can be proved that the function $f(z)$ has the following remarkable properties:

1. The function $f(z) - 1$ has zeros at the points z_{cen} (and only at these points)—the centres of zero-angled triangles tessellating the Poincaré hyperbolic upper half-plane $\mathcal{H}(z|\mathrm{Im}\, z > 0)$;
2. The function $f(z)$ has local maxima at all the points z_{cen} and only at these points.

All the solutions of the equation $f(z) - 1 = 0$ define all the coordinates of the 3-branching Cayley tree isometrically embedded into the upper half-plane $\mathcal{H}(z|\mathrm{Im}\, z > 0)$. The corresponding density plot of the function $f(z)$ in the region $\{0 \leqslant \mathrm{Re}\, z \leqslant 1, 0.04 \leqslant \mathrm{Im}\, z \leqslant 1.4\}$ is shown in figure 3. It is noteworthy that the function $Z(z) = [Cf(z)]^{-2}$ is the partition function of a free bosonic field on a torus [14]. The function $Z(z)$ has been extensively studied in conformal field theory.

The proof of the assertion is based on the classical relation for the Dedekind function [13]

$$\eta\left(\frac{pz + r}{qz + s}\right) = \omega\sqrt{qz + s}\,\eta(z) \tag{8}$$

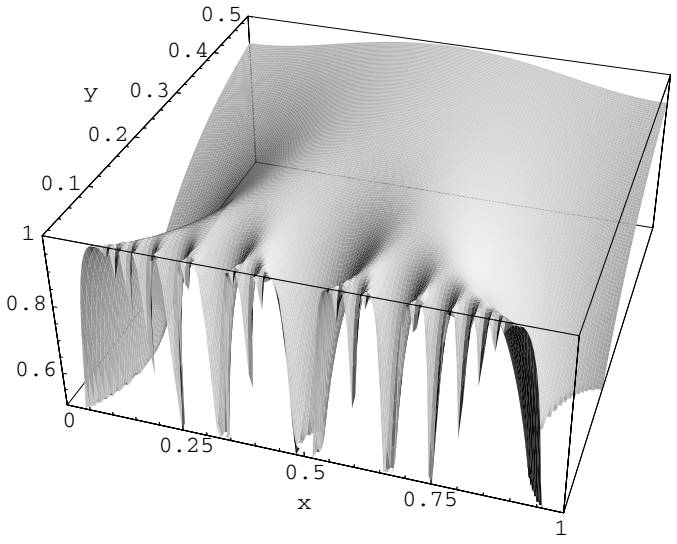

Figure 3. Relief of the function $f(z)$ in the rectangle $\{0 \leqslant \mathrm{Re}\, z \leqslant 1, 0.04 \leqslant \mathrm{Im}\, z \leqslant 1.4\}$.

where $\mathrm{Im}\, z > 0, \{p, q, r, s\} \in Z$; $ps - qr = 1$ and ω is some 24-power root of unity, which depends on the coefficients p, q, r, s but does not depend on z. Using (8) and the definition (6), (7), we have

$$\begin{cases} f(z+1) = f(z) \\ f\left(-\dfrac{1}{z}\right) = f(z) \\ f(-\bar{z}) = f(z). \end{cases} \tag{9}$$

The properties 1 and 2 of our assertion follow directly from (9).

Let us note the important duality relation for the function $f(z)$ defined in (6) which establishes the mapping $y \leftrightarrow \frac{1}{y}$ (where $y = \mathrm{Im}\, z$; $y > 0$). For all $\{p, q, r, s\} \in Z$ such that $ps - qr = 1$ the following equation is satisfied:

$$f\left(\left\{\frac{p}{q}\right\} + \mathrm{i}y\right) = f\left(\left\{\frac{s}{q}\right\} + \frac{\mathrm{i}}{q^2 y}\right) \tag{10}$$

where by $\left\{\frac{p}{q}\right\}$ and $\left\{\frac{s}{q}\right\}$ we denote the fractional parts of the corresponding quotients. The relation (10) shall be used in the following sections for practical purposes of numerical computations. In the following section we discuss the ultrametric organization of corresponding barriers. We regard the 3D relief constructed on the basis of the function $f(z)$ (see figure 3) as the continuous analogue of the Cayley tree isometrically embedded in $\mathcal{H}(z|\mathrm{Im}\, z > 0)$.

2.2. Ultrametric structure of barriers in the standard RSB scheme and in the tree-like metric space

The RSB scheme [5] has appeared in the spin-glass theory as a self-consistent approach free from many shortcomings of the replica symmetric consideration. Later on it was realized that the RSB structure naturally appears in the problem of diffusion on the boundary of the Cayley tree [15, 16], where the neighbouring sites are separated by the barriers hierarchically

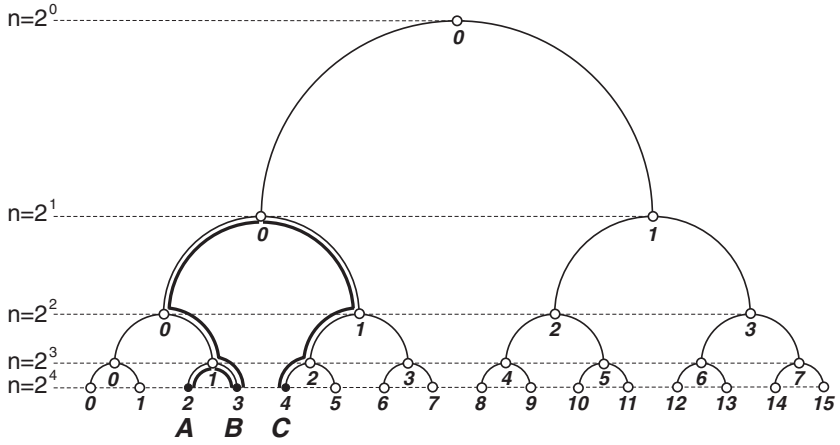

Figure 4. The 3-branching Cayley tree. The ultrametric distance between points A, B and B, C is shown by bold lines; n is the number of states in each generation of the tree, the maximal number of generations $L = 4$.

organized according to their ultrametric distances on the Cayley tree. For example, the neighbouring points A, B and B, C at the boundary of the 3-branching Cayley tree (see figure 4) are separated by the barriers depending on the ultrametric distance between points A, B and B, C on the tree.

Recall that two points, say, B and C in figure 4, are separated by the potential barrier depending on the number of the Cayley tree generations from the points B and C up to their common 'parent branch'. Let us label the states at the L generation of the 3-branching Cayley tree by the integer number k ($1 \leqslant k \leqslant 2^L$). If we represent k by the binary sequence, then the ultrametric distance between points B and C shall coincide with the highest distinct rank in the binary writing of $k_B = 4$ and $k_C = 5$.

Denote by q_m the Boltzmann weights at the boundary of the 3-branching Cayley associated with the barriers of ultrametric height m. All the barriers can be encoded in the $2^L \times 2^L$ RSB matrix $\mathbf{Q}(q_0, q_1, \ldots, q_L)$ having the structure shown in equation (11) for $L = 3$. Keeping in mind the relation with spin glasses, the total number of states 2^L is associated with the total number of replicas, n, in the standard RSB scheme.

$$\mathbf{Q} = \left[\begin{array}{cccc|cccc|cccc|cccc} q_0 & q_1 & q_2 & q_2 & q_3 & q_3 & q_3 & q_3 \\ q_1 & q_0 & q_2 & q_2 & q_3 & q_3 & q_3 & q_3 \\ \hline q_2 & q_2 & q_0 & q_1 & q_3 & q_3 & q_3 & q_3 \\ q_2 & q_2 & q_1 & q_0 & q_3 & q_3 & q_3 & q_3 \\ \hline q_3 & q_3 & q_3 & q_3 & q_0 & q_1 & q_2 & q_2 \\ q_3 & q_3 & q_3 & q_3 & q_1 & q_0 & q_2 & q_2 \\ \hline q_3 & q_3 & q_3 & q_3 & q_2 & q_2 & q_0 & q_1 \\ q_3 & q_3 & q_3 & q_3 & q_2 & q_2 & q_1 & q_0 \end{array}\right]. \tag{11}$$

The values $p_m = \frac{1}{n} q_m$ ($m = 1, \ldots, L$) define the jumping probabilities from some vertex k_1 to another vertex k_2 at the boundary of 3-branching Cayley tree separated by the barrier of ultrametric height m, while the value p_0 is assigned for the probabilities to stay in a given vertex. In each line of the matrix $\mathbf{Q}$ the sum of probabilities is equal to 1. In most

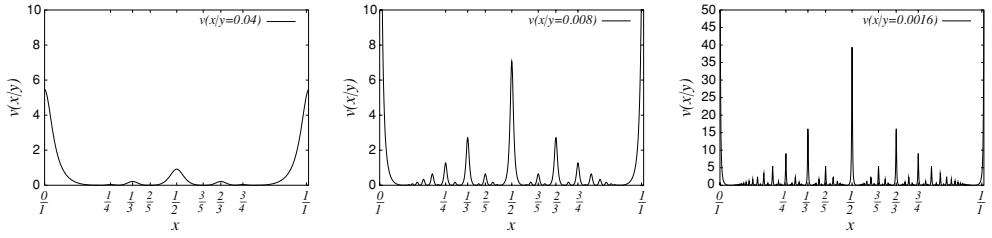

Figure 5. Typical shape of the function $v(x|y) = -\ln f(x|y)$ for a few values $y = 0.04$, $0.008, 0.0016$.

physically important situations the Boltzmann weights q_m depend on m either exponentially or polynomially:

$$q_m = \begin{cases} \text{const } m^{\alpha} \\ \text{const } \mathrm{e}^{-\beta m}. \end{cases} \tag{12}$$

Later on we pay attention only to the exponential dependence of q_m on m, i.e. to the case when $q_m = \text{const } \mathrm{e}^{-\beta m}$ (where β stands for the inverse temperature). The probability p_0 of staying in a given vertex can be explicitly computed from the conservation condition $\sum_{m=0}^{n} P_m = 1$ and for $q_m = \text{const } \mathrm{e}^{-\beta m}$ it reads

$$p_0 = 1 - \frac{1}{n}\sum_{j=1}^{L} 2^j \,\mathrm{e}^{-\beta j} = 1 - \frac{2\mathrm{e}^{-\beta}(1-(2\mathrm{e})^{-\beta L})}{n(1-(2\mathrm{e})^{-\beta})} \tag{13}$$

In order to understand the relation between the ultrametric structure of the barriers in the case of a 3-branching Cayley tree and its continuous analogue isometrically embedded in $\mathcal{H}(z|\mathrm{Im}\, z > 0)$, let us begin with the following observation. We can consider the function $v(x|y) = -\ln f(x|y)$ (where $x = \mathrm{Re}\, z$) as the potential relief at the boundary of the Cayley tree cut at the distance $y = \mathrm{Im}\, z$ from the real axis. The typical shapes of the function $v(x|y)$ for a few fixed values $y = 0.04, 0.008, 0.0016$ are shown in figure 5. This picture clearly demonstrates the ultrametric organization of the barriers separating the valleys.

As one can see in figure 5, the distance from the real axis, y, characterizes the number of Cayley tree generations: the closer the value y to the real axis, the more new generations of barriers appear (and the higher the barriers). The relation of the system of barriers shown in figure 5 with the structure of RSB matrix (11) becomes very straightforward now. The barriers of smallest scale correspond to the values q_1 in the matrix $\mathbf{Q}(q_0, q_1, \ldots, q_L)$, the barriers of the next scale correspond to q_2 etc. Hence, the distance y may be considered as the parameter controlling the size of the RSB matrix: as $y \to 0$ the size of $\mathbf{Q}$ tends to infinity. Thus, one can conjecture that the number of the replicas, n, is a function of y. This relation shall be discussed at length in the following section.

The function $v(x|y) = -\ln f(x|y)$, defined on the interval $0 < x < 1$, has the properties borrowed from the structure of the underlying modular group $PSL(2, \mathbb{Z})$ acting in the half-plane $\mathcal{H}(z|y > 0)$ [17, 18]. In particular:

- the local maxima of the function $v(x)$ are located at the rational points;
- the highest barrier on a given interval $\Delta x = [x_1, x_2]$ is located at a rational point $\frac{p}{q}$ with the lowest denominator q. On a given interval $\Delta x = [x_1, x_2]$ there is only one such point. The locations of the barriers with consecutive heights on the interval Δx are organized according to the group operation:

$$\frac{p_1}{q_1} \oplus \frac{p_2}{q_2} = \frac{p_1 + p_2}{q_1 + q_2}. \tag{14}$$

Figure 5 clarifies this statement. The highest barriers on the interval $0 \leqslant x \leqslant 1$ are located at the points $x_0 = 0$ and $x_1 = 1$. Rewriting 0 and 1 correspondingly as $\frac{0}{1}$ and $\frac{1}{1}$ we can find the point x_2 of the location of the barrier with the next maximal hight. Namely, $x_2 = \frac{0}{1} \oplus \frac{1}{1} = \frac{0+1}{1+1} = \frac{1}{2}$. Continuing this construction we arrive at the hierarchical structure of barriers located at rational points organized in the Farey sequence. According to our construction this should replace the standard RSB scheme. The corresponding 'modular' (MRSB) matrix shall be constructed in the following section.

2.3. Explicit organization of barriers on the basis of Dedekind function

The above discussion gives an idea of the construction. However, to establish the precise connection between the standard RSB scheme and the 'number-theoretic' MRSB scheme, we should construct the MRSB scheme with exponential organization of the Boltzmann weights—as in RSB. Recall that the ultrametric distance between two points A and B on the Cayley graph is equal to one half of the number of steps of the shortest path connecting these points. For example, the ultrametric distances r_{AB} (between points A and B) and r_{AC} (between points A and C) in figure 4 are as follows: $r_{AB} = 1$ and $r_{AC} = 3$. It is clearly seen that the points A and B (as well as the points B and C) are separated by the barrier located at point $x_1 = \frac{1}{3}$, while the points A and B are separated by the barrier located at the point $x_2 = \frac{2}{7}$. According to the last equation of (12), the height U_m of the barrier between two points separated by the ultrametric distance m in the standard RSB scheme reads

$$U_{\mathrm{RSB},m} \equiv -\ln q_m = \beta m. \tag{15}$$

The dependence of Boltzmann weights on the ultrametric distance in the MRSB scheme should also satisfy (15). This implies that the heights U_{MRSB} of the MRSB barriers should linearly depend on the ultrametric distance between two vertices of the Cayley tree. To adjust the heights of the barriers in MRSB and RSB schemes some auxiliary work has to be done. The corresponding construction is described in the rest of this section.

Begin with the standard RSB tree and distribute barriers separating all 2^L boundary points of the Cayley tree in the generation L equidistantly in the unit interval [0, 1]. For example, for $L = 1$ there are two vertices of the Cayley tree separated by a single barrier located at the point $x_1 = \frac{1}{2}$. The barriers of the second generation $L = 2$ are placed at the points $x_2^{(1)} = \frac{1}{4}$ and $x_2^{(2)} = \frac{3}{4}$. For $L = 3$ we have $x_3^{(1)} = \frac{1}{8}$, $x_3^{(2)} = \frac{3}{8}$, $x_3^{(3)} = \frac{5}{8}$, $x_3^{(3)} = \frac{7}{8}$ etc. The points $x_L^{(j)} = \frac{j}{2^L}$ (where j is odd and $1 < j < 2^L$) cover uniformly the unit interval [0, 1]. Let us normalize the barrier heights as follows. In the finite Cayley tree of L generations there are 2^{L-1} *smallest* barriers; all of them have equal heights. Let these barriers be of height $U(L) = \frac{1}{L}$. Then the *averaged* barriers in some intermediate generation m ($1 \leqslant m \leqslant L$) have the height

$$U(m, L) = \frac{L - m + 1}{L} \equiv 1 - \frac{m - 1}{L}. \tag{16}$$

Hence, in the first generation $m = 1$ the height of a single barrier located at the point $x_1 = \frac{1}{2}$ is normalized by 1: $U(m = 1, L) = 1$. This sets our normalization condition. Let us note that the choice of the normalization of the barriers might be considered as the renormalization of the inverse temperature $\beta \to \tilde{\beta} L$ (see (15)). The 'physical' sense of such renormalization consists in the following. When the number of Cayley tree generations L is increased, the corresponding landscape acquires more small scale details without changing the height of the maximal barrier, which is always normalized by 1.

Now we proceed in a similar way with the continuous MRSB structure. Recall that the logarithm of the Dedekind function has maxima at the rational points $x = \frac{p}{q}$. The set of these points $\{x_i\}$ can be generated recursively as has been explained above in connection with

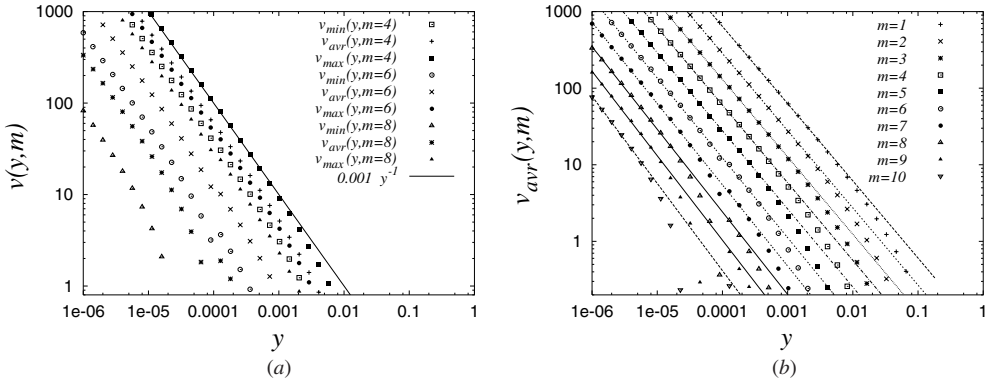

Figure 6. (*a*) Minimal $v_{\min}(y)$, average $v_{\mathrm{avr}}(y)$ and maximal $v_{\max}(y)$ barriers for $m = 4, 6, 8$; (*b*) the function $v_{\mathrm{avr}}(y)$ for $m = 1, \ldots, 10$.

equation (14). We start with two 'parent' points $0 = \frac{0}{1}$ and $1 = \frac{1}{1}$ of zero's generation. In the first step we generate a barrier at the point $\frac{1}{r2} = \frac{0+1}{1+1}$; in the second step we generate two barriers at the points $\frac{1}{3} = \frac{0+1}{1+2}$ and $\frac{2}{3} = \frac{1+1}{2+1}$ and so on. We shall call the number of recursive steps necessary to arrive at a barrier located at a specific point $x = \frac{p}{q}$ *the generation* in which this barrier has appeared for the first time. Let us fix the maximal generation L. Define $\{x_i\}(m)$ the set of points in the generation $m \leqslant L$ at which the barriers are located. There are 2^{m-1} such points. For example, $\{x_i\}(m = 1) = \left\{\frac{1}{2}\right\}$, $\{x_i\}(m = 2) = \left\{\frac{1}{3}, \frac{2}{3}\right\}$, $\{x_i\}(m = 3) = \left\{\frac{1}{4}, \frac{2}{5}, \frac{3}{5}, \frac{3}{4}\right\}$ and so on. Now we need to express the heights $U_{\mathrm{MRSB}}(x_i, m, y)$ of the barriers up to the generation $m \leqslant L$ via the Dedekind function $\eta(x_i, y)$. Take the logarithm of the normalized Dedekind function

$$v(x|y) = -\ln f(x|y) \tag{17}$$

as the possible basis for such construction (the function $f(x, y)$ is defined in (6)). Our choice is justified by the fact that this function has maxima at the points $\{x_i\}(m)$ and demonstrates the ultrametric behaviour. Starting from $m \geqslant 3$, the values of the function $v(x_i, m|y)$ at the points of maxima $\{x_i\}(m)$ do not become equal. In figure 6(*a*) we have plotted the minimal $v_{\min}(m|y) = \min(v(x_i, m|y))$, the average $v_{\mathrm{avr}}(m|y) = \langle v(x_i, m|y)\rangle$ and the maximal $v_{\max}(m|y) = \max(v(x_i, m|y))$ barrier heights in each of the three generations $m = 4, 6, 8$. The brackets $\langle\cdots\rangle$ denote averaging over all barriers in the generation m. The function $0.001\,y^{-1}$ is plotted for comparison in the same figure.

Figure 6(*a*) allows us to conclude that $v(m|y) \sim y^{-1}$ for fixed m. More detailed information about the function $h_{\mathrm{avr}}(m|y) = \langle -\ln(\eta(x_i|y))\rangle$ can be extracted from figure 6(*b*), which is similar to 6(*a*) but is extended up to $m \in [1, 10]$. The data shown in figure 6(*b*) are approximated by the natural fit

$$v_{\mathrm{avr}} = a_m y^{b_m}$$

for all points such that $v_{\mathrm{avr}} > 10$. The results of our approximation are shown in table 1 as well as drawn in figure 6(*b*) by lines.

We have plotted the coefficient a_m as a function of m in figure 7(*a*). The approximation $a_m \simeq 0.144(8)\,\mathrm{e}^{-0.847(18)m}$ is shown in the same figure by the dashed line. Hence, we expect the following relation $v(m|y) \simeq 0.144(8)\,\mathrm{e}^{-0.847(18)m}\,y^{-1}$.

The analysis of the numerical data for the averaged logarithm of the Dedekind function allows us to conjecture the general ansatz

$$v_{\mathrm{avr}}(m|y) \equiv \langle -\ln f(x_i|y)\rangle = \mathrm{d}(y)\,\mathrm{e}^{-c(y)m}\,y^{-1}. \tag{18}$$

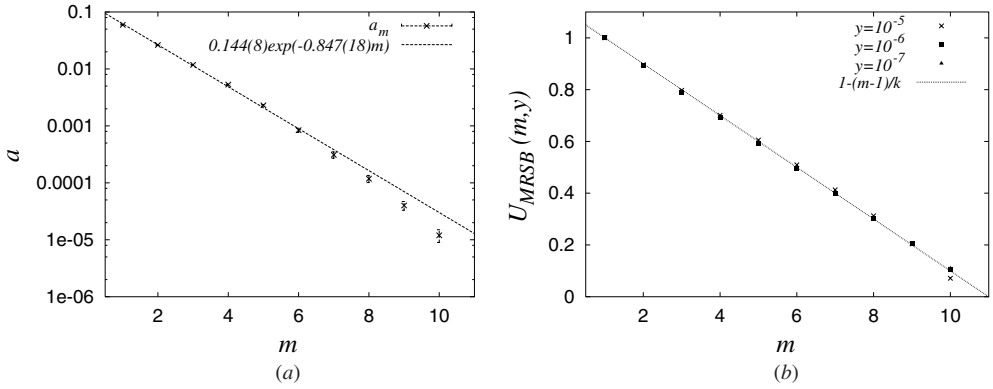

Figure 7. (*a*) Approximation of the coefficient a_m; (*b*) ultrametric barriers $U_{\mathrm{MRSB}}(m|y) = \frac{1}{c(y)L} \ln \frac{v(m|y))}{v(1,y)}$.

Table 1. Numerical results of the fit $v_{\mathrm{avr}} = a_m y^{b_m}$.

m	a_m	b_m
1	0.0594(8)	−1.008(2)
2	0.0263(4)	−1.008(1)
3	0.0118(2)	−1.011(1)
4	0.0053(1)	−1.014(2)
5	000230(7)	−1.021(3)
6	0.00084(7)	−1.04(1)
7	0.00031(4)	−1.06(1)
8	0.000118(17)	−1.08(6)
9	0000040(7)	−1.102(1)
10	0000012(3)	−1.14(2)

This equation establishes the functional dependence of the average height v_{avr} on the generation m ($m = 1, 2, \ldots$) for fixed y. Recall that the generation m is defined as the minimal number of recursive steps necessary to arrive at a barrier located at a specific point $x_i = \frac{p}{q}$. Let us now fix the maximal generation L. Our desire is to obtain the normalized barrier for the MRSB scheme as has been done for RSB (see equation (16)). Taking into account that (18) is valid for any $m \geqslant 1$, we may extract m from (18) and write it as follows:

$$m = 1 + \frac{1}{c(y)} \ln \frac{v_{\mathrm{avr}}(m|y)}{v_{\mathrm{avr}}(m = 1|y)}. \tag{19}$$

Substituting (19) into (16) we get the following formal expression for the height of the barriers in the MRSB scheme:

$$U_{\mathrm{MRSB}}(x_m, L|y) \equiv 1 - \frac{m-1}{L} = 1 + \frac{1}{c(y)L} \ln \frac{v_{\mathrm{avr}}(m|y)}{v_{\mathrm{avr}}(1|y)}. \tag{20}$$

Now we should explain how it is possible to use the formal equation (20) in practical computations. Let us fix the maximal generation L and define the value y^* from the equation

$$v_{\mathrm{avr}}(L|y^*) = 1. \tag{21}$$

The value y^* has the following sense. For all $y < y^*$ the value $v_{\mathrm{avr}}(m|y)$ does not depend on m ($m \leqslant L$) because all barriers in the generation m are already presented and hence the

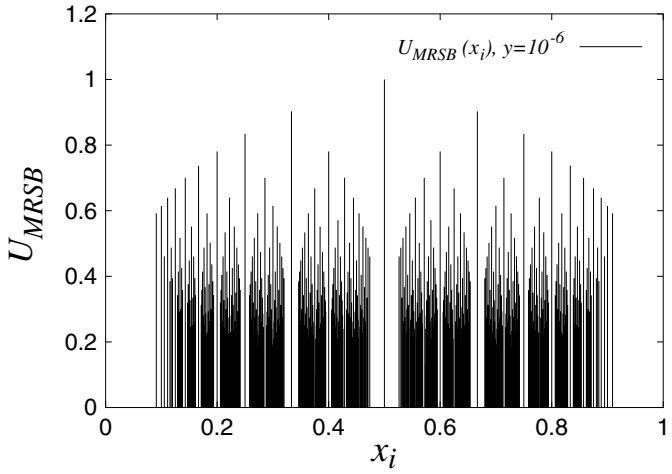

Figure 8. Ultrametric barriers $U_{\mathrm{MRSB}}(x_i)$ at the rational points x_i for $y = 10^{-6}$.

Table 2. Dependence of the parameter $c(y)$ on $y = y^*$ up to $L = 10$ generations (see equation (22)).

y^*	$c(y^*)$
5.12×10^{-5}	0.820(11)
2.56×10^{-5}	0.8057(99)
1.28×10^{-5}	0.7944(86)
6.4×10^{-6}	0.7718(29)
3.2×10^{-6}	0.7623(22)
1.6×10^{-6}	0.7579(27)
8×10^{-7}	0.7556(30)
4×10^{-7}	0.7544(32)
2×10^{-7}	0.7538(37)
1×10^{-7}	0.7535(34)

average height v_{avr} cannot be changed for any $y < y^*$. Therefore we can postulate, that for all $y < y^*$ the height of the barrier is described by the function

$$U_{\mathrm{MRSB}}(x_i) = 1 + \frac{1}{c(y^*)L} \ln \frac{\ln f(x_i|y^*)}{\ln f\left(\frac{1}{2}\middle|y^*\right)} \tag{22}$$

where x_i is the rational point of the barrier location and we have used (17). The discussion of the dependence $c(y^*)$ deserves special attention. As shown in table 2, for sufficiently small y^* the value of c tends to a constant value. Thus the function $U_{\mathrm{MRSB}}(x_i)$ defines the heights of ultrametric barriers in the MRSB scheme fully consistent with the heights of the RSB barriers for the Cayley tree. It should be noted that for intermediate values of y some barriers of large generations are negative due to the cut (21), however for any fixed m, we can always find y^* such that all barriers are positive. For example, for $y \leqslant y^* = 10^{-6}$ all barriers up to $m = 10$ generations are positive.

Our tedious but simple construction is clearly explained in figure 8, where we have plotted the heights of barriers $U_{\mathrm{MRSB}}(x_i)$ at the rational points x_i up to the generation $L = 10$ for $y^* = 10^{-6}$. Once the maximal generation L is fixed and all barriers for all generations

(up to the maximal one) are shown in the picture, then this picture is unchanged for all y such that $y < y^*$. According to our definition, these barriers are normalized in such a way that the height of the largest barrier is equal to 1. The average height of the barriers of the second (third, fourth, etc) generation is equal to 0.9 (0.8, 0.7, etc)—compare to (16). Let us repeat that in figure 8 we have displayed the barriers corresponding to generations m up to $m = L$. We can easily relax this condition and work with the set of *all* possible barriers up to some fixed minimal value $y_{\min}$ without paying attention to how many generations are counted.

2.4. Description of dynamical models

Our aim is to investigate numerically the probability distribution of a random walk on the boundary of an ultrametric space. This problem was a subject of the original work [15] where the dynamics in the ultrametric space was considered in the framework of the discrete model of jumps on the boundary of a 3-branching Cayley tree. The first application of p-adic analysis for the computation of the probability distribution of the diffusion at the boundary of the ultrametric tree was successfully realized in [6]. Below we reconsider the diffusion problem in the continuous metric space, where the ultrametric organization of the barriers is due to the modular structure of the Dedekind function. The advantages of such consideration we shall discuss in the conclusion. Let us specify the models under consideration.

2.4.1. The standard RSB model. In this model we consider the random jumps at the boundary of a 3-branching Cayley tree (see figure 4). The transition probabilities between the Cayley tree vertices are encoded in the matrix (11). As explained above, we fix the total number of generations L and set the highest barrier (in the first generation) always equal to 1. Then the heights of the barriers of generation m are given by (16), while the height of the smallest barriers in the generation L is equal to $\frac{1}{L}$. Increasing the number of generations L, we increase the resolution of our model without changing the value of the maximal barrier. We use this problem of diffusion on the boundary of the standard 3-branching Cayley tree as a testing area for diffusion in the continuous tree-like ultrametric space.

Let $P_N(k, k_0)$ be the partition function of the random walk starting at the point k_0 and ending after N steps at the point k, where k labels the vertices of the k generation of the Cayley tree and both points k_0 and k belong to the m generation of the tree. The corresponding diffusion is governed by the recursion relation

$$\begin{cases} P^{\mathrm{RSB}}_{N+1}(k) = \displaystyle\sum_{k'=0}^{2^L-1} Q^{\mathrm{RSB}}(k,k')\,P^{\mathrm{RSB}}_{N}(k') \\ P^{\mathrm{RSB}}_{N=0}(k) = \delta_{k,k_0} \end{cases} \tag{23}$$

where $Q^{\mathrm{RSB}}(k, k')$ is the $2^L \times 2^L$ matrix whose elements are the Boltzmann weights associated with jumps from some point k_1 to the point k_2 ($\{k_1, k_2\} \in [1, 2^L]$) at the boundary of a 3-branching Cayley tree cut at the generation L. In order to take into account the ultrametricity of the Cayley tree, the matrix $Q^{\mathrm{RSB}}(k, k')$ should have the RSB structure and hence should coincide with the matrix $\mathbf{Q}$ in (11).

2.4.2. The quasi-continuous MRSB model. This model is defined as follows. We fix the maximal generation L and consider the heights of the potential U_{MRSB} (see (22)) corresponding to generations less than or equal to L. For example, in figure 9(a) we have plotted $15 = 2^L - 1 = n$ barriers up to $L = 4$ generation. The rational points x_i split the interval [0, 1] into 16 subintervals $[x_{i-1}, x_i]$, $i = 1, 2, \ldots, 15$ (including the subintervals

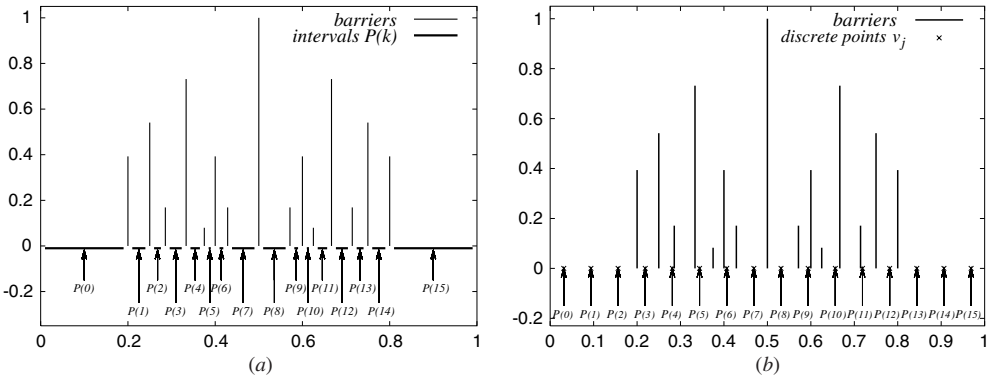

Figure 9. Location of barriers up to four generations. (*a*) Model I: the values v_i correspond to the intervals between maxima. (*b*) Model II: the values v_i correspond to the discrete points.

$[0, x_1]$ and $[x_{15}, 1]$). The random walker can jump from one interval to any other interval. Let us enumerate the intervals by the variable $k = 1, 2, 3, \ldots, 16$. So, $k = 1$ denotes the interval $[0, x_1]$, $k = 2$ is the interval $[x_1, x_2]$, etc.

Let $U_{\mathrm{MRSB}}(k, k')$ be the maximal barrier between the intervals k and k' defined by (22). By construction $U_{\mathrm{MRSB}}(k, k) = 0$. According to our rules, if $x \in [x_{k-1}, x_k]$ and $x' \in [x_{k'-1}, x_{k'}]$ then $U_{\mathrm{MRSB}}(x, x') = U_{\mathrm{MRSB}}(k, k')$. Thus we can write the recursive relation for the continuous distribution function $W_N(x)$. This function is defined for $x \in \mathbb{R}\,(0 \leqslant x \leqslant 1)$, where N enumerates the time moments. We claim for this quasi-continuous MRSB case the following form of the master equation which should replace equation (23):

$$\begin{cases} W_{N+1}(x) = \displaystyle\int_0^1 \mathrm{d}x'\, \mathrm{e}^{-\beta U_{\mathrm{MRSB}}(x,x')} W_N(x') \\ W_{N=0}(x) = \delta_{x,x_0}. \end{cases} \tag{24}$$

We can transform (24) making it more similar to (23). Namely, define $P_N^{\mathrm{MRSB}}(k)$, the probability that the walker belongs to the kth interval on the Nth jump (time step),

$$P_N^{\mathrm{MRSB}}(k) = \int_{x_{k-1}}^{x_k} W_N(x)\, \mathrm{d}x. \tag{25}$$

The normalization of the probability defines the sum over all intervals $\sum_{k=1}^{n} P_N^{\mathrm{MRSB}}(k) = \int_0^1 W_N(x)\, \mathrm{d}x = 1$. Integrating (24) over the interval [0, 1] and replacing the integrals over $\mathrm{d}x$ and $\mathrm{d}x'$ by sums over k and k', we get

$$\begin{aligned} \sum_{k=1}^{n} P_{N+1}^{\mathrm{MRSB}}(k) &= \int_0^1 W_{N+1}(x)\, \mathrm{d}x = \int_0^1 \int_0^1 \mathrm{e}^{-\beta U_{\mathrm{MRSB}}(x,x')} W_N(x')\, \mathrm{d}x'\, \mathrm{d}x \\ &= \sum_{k=1}^{n} \sum_{k'=1}^{n} \int_{x_{k-1}}^{x_k} \int_{x'_{k'-1}}^{x'_{k'}} \mathrm{e}^{-\beta U_{\mathrm{MRSB}}(x,x')} W_N^{\mathrm{MRSB}}(k')\, \mathrm{d}x'\, \mathrm{d}x \\ &= \sum_{k=1}^{n} \sum_{k'=1}^{n} l_k\, \mathrm{e}^{-\beta U_{\mathrm{MRSB}}(k,k')} P_{k'}^{\mathrm{MRSB}} \end{aligned} \tag{26}$$

where l_k is the length of the kth interval $l_k = \int_{x_{k-1}}^{x_k} \mathrm{d}x = x_k - x_{k-1}$. Here we have used (25) to express $P_{N+1}^{\mathrm{MRSB}}(k)$ and $P_N^{\mathrm{MRSB}}(k')$ via $W_{N+1}^{\mathrm{MRSB}}(x)$ and $W_N^{\mathrm{MRSB}}(x')$. Now we can separate equations for different k and write

$$P_{N+1}^{\mathrm{MRSB}}(k) = \sum_{k'=1}^{n} Q(k,k') P_N^{\mathrm{MRSB}}(k') \tag{27}$$

where

$$Q(k,k') = l_k \, \mathrm{e}^{-\beta U_{\mathrm{MRSB}}(k,k')} \tag{28}$$

is the probability of jumping from the interval k' to the interval k. This probability is the product of the measure of the appropriate interval l_k and the Boltzmann weight $\mathrm{e}^{-\beta U_{\mathrm{MRSB}}(k,k')}$.

Define a vector $\mathbf{P}_N^{\mathrm{MRSB}}$ whose elements $P_N^{\mathrm{MRSB}}(k)$ are the probabilities for a walker to reach the interval k on the N jump. The vector $\mathbf{P}_0^{\mathrm{MRSB}}$ is the initial probability distribution on the intervals. Introduce a matrix $\mathbf{Q}$ with the elements $Q(k,k')$, and a matrix $\mathbf{U}_{\mathrm{MRSB}}$ with the elements $U_{\mathrm{MRSB}}(k,k')$. The elements of these two matrices are connected by the relation (28). The probability for the walker to reach the interval k at the time moment N is the k element of the vector $\mathbf{P}_N^{\mathrm{MRSB}}(k)$

$$\mathbf{P}_N^{\mathrm{MRSB}}(k) = \mathbf{Q}^N \mathbf{P}_0^{\mathrm{MRSB}}. \tag{29}$$

Let us recall that the barrier $U_{\mathrm{MRSB}}(k,k')$ between the points k and k' is the highest barrier on the interval $[k,k']$. Such barriers are located at the rational points $\{k_m\}$. This defines the ultrametric structure of the matrix $\mathbf{U}_{\mathrm{MRSB}}$ and, therefore, of $\mathbf{Q}$. By construction the matrix $\mathbf{U}_{\mathrm{MRSB}}$ reflects the ultrametric hierarchy of barriers appearing in the standard RSB matrix (see equation (11)). For example, the structure of the 'modular' MRSB matrix $\mathbf{U}_{\mathrm{MRSB}}$ defining the heights of the barriers between all the intervals along the x-axis for $L = 8$ is displayed below:

$$\mathbf{U}_{\mathrm{MRSB}} = \left(\begin{array}{cccc|cccc}
U_0 & U\left(\frac{1}{4}\right) & U\left(\frac{1}{3}\right) & U\left(\frac{1}{3}\right) & U\left(\frac{1}{2}\right) & U\left(\frac{1}{2}\right) & U\left(\frac{1}{2}\right) & U\left(\frac{1}{2}\right) \\
U\left(\frac{1}{4}\right) & U_0 & U\left(\frac{1}{3}\right) & U\left(\frac{1}{3}\right) & U\left(\frac{1}{2}\right) & U\left(\frac{1}{2}\right) & U\left(\frac{1}{2}\right) & U\left(\frac{1}{2}\right) \\
\hline
U\left(\frac{1}{3}\right) & U\left(\frac{1}{3}\right) & U_0 & U\left(\frac{2}{5}\right) & U\left(\frac{1}{2}\right) & U\left(\frac{1}{2}\right) & U\left(\frac{1}{2}\right) & U\left(\frac{1}{2}\right) \\
U\left(\frac{1}{3}\right) & U\left(\frac{1}{3}\right) & U\left(\frac{2}{5}\right) & U_0 & U\left(\frac{1}{2}\right) & U\left(\frac{1}{2}\right) & U\left(\frac{1}{2}\right) & U\left(\frac{1}{2}\right) \\
\hline
U\left(\frac{1}{2}\right) & U\left(\frac{1}{2}\right) & U\left(\frac{1}{2}\right) & U\left(\frac{1}{2}\right) & U_0 & U\left(\frac{3}{5}\right) & U\left(\frac{2}{3}\right) & U\left(\frac{2}{3}\right) \\
U\left(\frac{1}{2}\right) & U\left(\frac{1}{2}\right) & U\left(\frac{1}{2}\right) & U\left(\frac{1}{2}\right) & U\left(\frac{3}{5}\right) & U_0 & U\left(\frac{2}{3}\right) & U\left(\frac{2}{3}\right) \\
U\left(\frac{1}{2}\right) & U\left(\frac{1}{2}\right) & U\left(\frac{1}{2}\right) & U\left(\frac{1}{2}\right) & U\left(\frac{2}{3}\right) & U\left(\frac{2}{3}\right) & U_0 & U\left(\frac{3}{4}\right) \\
U\left(\frac{1}{2}\right) & U\left(\frac{1}{2}\right) & U\left(\frac{1}{2}\right) & U\left(\frac{1}{2}\right) & U\left(\frac{2}{3}\right) & U\left(\frac{2}{3}\right) & U\left(\frac{3}{4}\right) & U_0
\end{array}\right). \tag{30}$$

2.4.3. The discretized MRSB model. In this model the location of the barriers is the same as in model II, but now we split the total interval [0, 1] into $n = 2^L$ subintervals of equal length $\frac{1}{n}$ each. The midpoint of the kth interval is the point $\bar{x}_k = -\frac{1}{2n} + \frac{k}{n}$. We consider the distance between intervals k and k' as the distance between the midpoints: $U_{\mathrm{III}}(k,k') = U_{\mathrm{MRSB}}(\bar{x}_k, \bar{x}_{k'})$. Namely, we consider jumps between n midpoints $k\,(k = 1, 2, \ldots, n)$ with coordinates $\bar{x}_k = -\frac{1}{2n} + \frac{k}{n}$.

The probability of jumping from a point k' to a point k is defined by the relation

$$Q^{\mathrm{III}}(k,k') = \frac{1}{L} \, \mathrm{e}^{-\beta U_{\mathrm{MRSB}}(\bar{x}_k, \bar{x}_{k'})}. \tag{31}$$

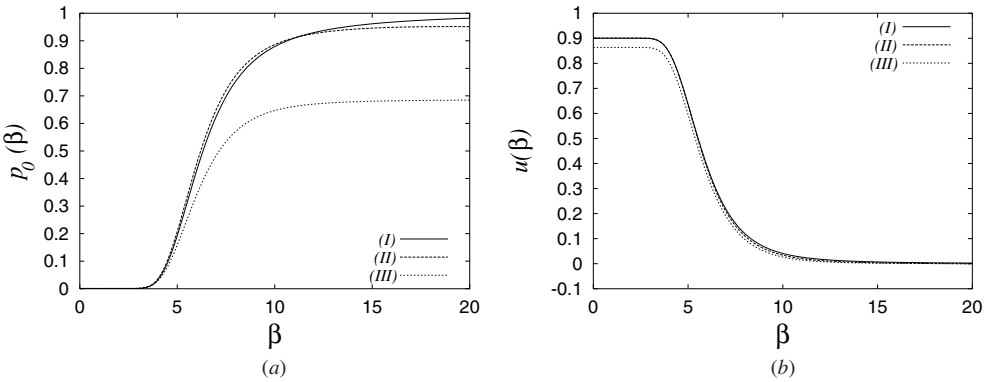

Figure 10. (*a*) $P_0(\beta)$; (*b*) $U(\beta)$. Numerical values of the parameters are: $L = 10$, $N = 400$.

Each element $P_N^{\mathrm{III}}(k)$ of the probability vector $\mathbf{P}$ corresponds to a point. In this model all barriers $x_i = \frac{p_i}{q_i}$ lie between the midpoints (see figure 9(*b*)). By comparing the models II and III it is easy to understand that the number n of points $\bar{x}_k$ in the interval between barriers $[x_k, x_{k+1}]$ plays the role of the measure of that interval.

Below we compare the numerical solutions of models I, II and III. To be more specific, we consider simultaneously the N-step random walk on the Cayley tree (model I) and on its continuous analogue (models II and III). First of all, we calculate the elements $[\mathbf{Q}^N](i, j)$ of the matrix $\mathbf{Q}^N$ for all three models. Then we compute:

- The probability P_0 of staying at the initial point after N random jumps

$$P_0 = \sum_{i=1} [\mathbf{Q}^N](i, i) \tag{32}$$

- The average ultrametric distance U between the initial and the final points of the N-step random walk:

$$U = \sum_{i=1}^{n} \sum_{j=1}^{n} [\mathbf{U}](i, j)[\mathbf{Q}^N](i, j) \tag{33}$$

  where $[\mathbf{U}](i, j)$ is the element of the matrix $\mathbf{U}$ defining the ultrametric distances between all available points. The sizes of the matrices $\mathbf{U}$ and $\mathbf{Q}$ are $n = 2^L$, where L is the total number of generations.

2.5. Numerical results for models I, II, III

The following three cases are studied numerically:

1. We fix the maximal generation, L, and the number of jumps, N, and plot P_0 and U as functions of the inverse temperature β (see figures 10(*a*), (*b*)) for the following numerical values of L and N: $L = 10$, $N = 400$.
2. We fix the maximal generation, L, and the inverse temperature, β, and plot P_0 and U as functions of the number of steps N (see figures 11(*a*), (*b*)) for the numerical values of L and β: $L = 10$, $\beta = 4$.
3. We fix the number of jumps, N, and the inverse temperature, β, and plot P_0 and U as functions of the maximal generation L (see figures 12(*a*), (*b*)) for the following numerical values of N and β: $N = 400$, $\beta = 1$.

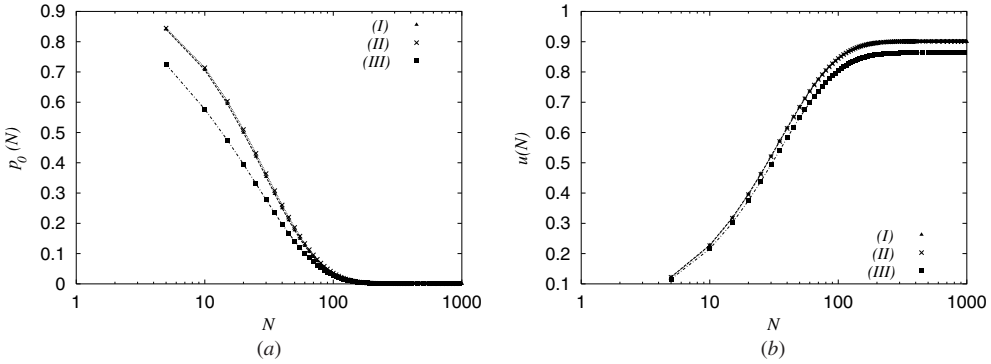

Figure 11. (*a*) $P_0(N)$; (*b*) $U(N)$. Numerical values of the parameters are: $L = 10$, $\beta = 4$.

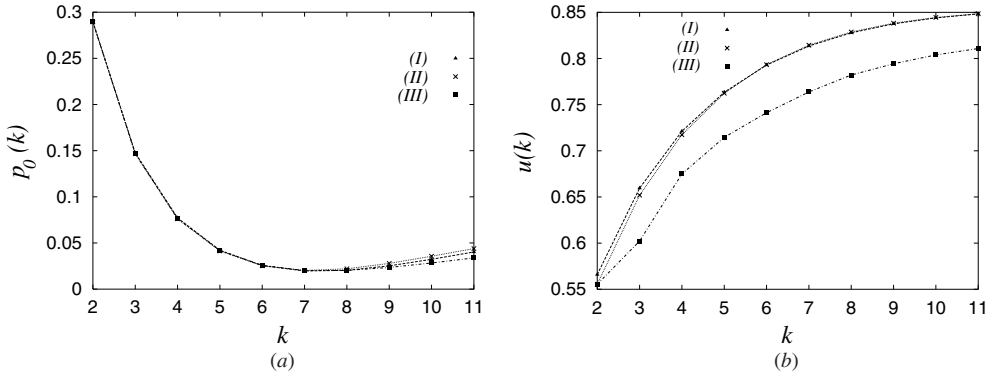

Figure 12. (*a*) $P_0(L)$; (*b*) $U(L)$. Numerical values of the parameters are: $N = 400$, $\beta = 1$.

3. Discussion

The numerical solutions of the master equations (23) and (24) shown in figures 10–12 allow us to conclude that we arrive at the same results for the return probability P_0 and the mean height of the barriers U for random walks in the ultrametric spaces independent of which model we consider: either the ultrametric structure of the barriers is defined on the boundary of the Cayley tree (case I), or the heights of these barriers are given by the properly normalized Dedekind function (cases II and III).

Our results are obtained under the condition that the heights of the ultrametric barriers in all models (I, II and III) have *linear dependence* on the number of Cayley tree generation. Recall that the construction of our ultrametric potential (22) on the basis of the Dedekind modular function is conditioned only by this demand. The current choice of the potential is stipulated basically for demonstrational aims. Namely, we have shown that it is possible to adjust the ultrametric structure of the continuous metric space $\mathcal{H}$ to the structure of the standard Cayley tree in such a way that we can mimic the main statistical properties of the random walk at the boundary of the Cayley tree by the diffusion in $\mathcal{H}$.

The key ingredient of our construction is the replacement of the RSB scheme (11) by the new MRSB scheme (30). Despite the fact that the corresponding master equation (24) allows only numerical treatment, the proposed construction, in our opinion, has some advantages with respect to the RSB scheme resulting from: (i) the self-duality (see equation (10)),

and (ii) the continuity of MRSB. We permit ourselves below to touch on both these properties (i) and (ii) in connection with the possible simplification of the solution of the continuous analogue of the master equation (26) (see section 3.1 below), and with the speculation about the geometry of the $n \to 0$ limit (see section 3.2 below). We clearly realize that the last subject is one of the most intriguing questions in the statistical physics of disordered systems, and our conjecture may be criticized from different points of view, however we believe that our geometric construction may stimulate the readers to fill the standard mode of thinking about the replicas by some fresh geometric sense.

It is worth saying a few words concerning the particular choice of the function considered as the 'continuous analogue' of the Cayley tree. Besides the Dedekind function there is a family of other functions which can be easily constructed. One example of such a 'continuous tree' is given below:

$$g_n(x|y) \sim \sum_{k=1}^{n} \sum_{j=1}^{2^k-1} \frac{1}{ky} \exp\left(-\frac{k^2(x-j/2^k)^2}{2y^2}\right).$$

Despite the function $g_n(x|y)$ resembling (to some extent) the relief shown in figure 3, this function $g_n(x|y)$ does not possess important number-theoretic properties (such as, for example, the self-duality exploited in our work). Moreover, the uniqueness of the function $f(z)$ (see equation (6)) becomes extremely transparent when considering the statistical models (such as ageing processes) on the whole Cayley tree, and not only at its boundary—in this case the isometric embedding of the tree in the surface built on the basis of the Dedekind function becomes very important.

3.1. The continuous MRSB model

Taking advantage of our construction of an ultrametric system of barriers described by the potential $U_{\mathrm{MRSB}}(x_m)$ (see (22)), we can replace the master equation (23) by its analogue based on the properties of the Dedekind function. The distribution function $W_N(x)$ is described by (24) where x_m is the rational point on the interval $[x', x]$ with the smallest denominator (there is only one such point). As we have already seen, the highest barrier $U_{\mathrm{MRSB}}(x_m)$ on the interval $[x', x]$ is located at the point x_m. The number of barriers and their heights are controlled simultaneously by the parameter y. As $y \to 0$, more new barriers appear. Gradually they become higher and narrower preserving the ultrametric structure. In this section we are interested in the limit $y \to 0$, where the hierarchical structure of barriers is highly developed (see, for example, figure 8). Simplification of equation (24) is allowed by using equation (10). Making in equation (24) the substitution which maps y to $\frac{1}{y}$ we obtain

$$U_{\mathrm{MRSB}}(x_m, y, L^*) \equiv 1 + \frac{1}{cL^*(y)} \ln \frac{\ln f(x_m, y)}{\ln f\left(\frac{1}{2}, y\right)}\bigg|_{y\to 0} \simeq 1 + \frac{2}{cL^*(y)} \ln \frac{2}{q} \tag{34}$$

where $L^*(y)$ is determined again using the relation (21). Equation (34) is valid only for $\{p, q, s, r\} \in \mathbb{Z}$ such that $ps - qr = 1$ (where r may be an arbitrary integer). The point $x_m = \left\{\frac{p}{q}\right\}$ and its 'dual image' $x'_m = \left\{\frac{s}{r}\right\}$ lie in the unit interval $[0, 1]$. Substituting (34) into (24), we have:

$$\begin{cases} W_{N+1}(x) = \displaystyle\int_0^1 \mathrm{d}x'\, \mathrm{e}^{-\beta} \left(\frac{2}{q}\right)^{2\beta/(cL^*(y))} W_N(x') \\ W_{N=0}(x) = \delta_{x,x_0}. \end{cases} \tag{35}$$

Equation (35) has a rich number-theoretic structure. In fact, the information on the position of the highest barrier in the interval $[x', x]$ is hidden in the integer q. Let us recall that the value

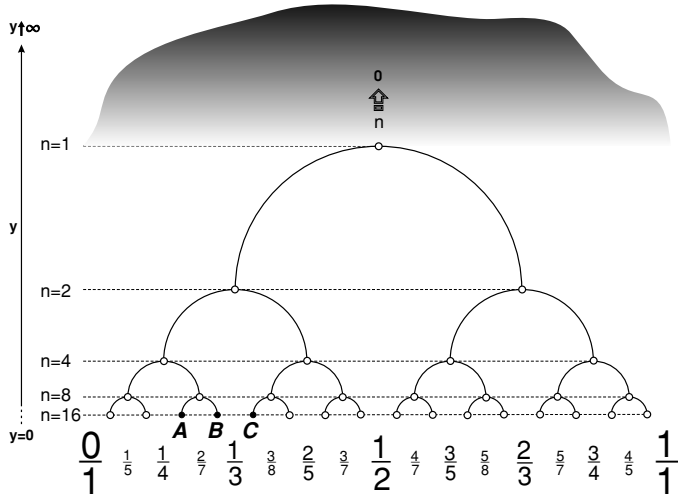

Figure 13. The 3-branching Cayley tree. The barriers are located at the rational points ordered in the Farey sequence. The replica limit $n \to 0$ is interpreted as the absence of states (vertices of the tree) when $y \to \infty$.

of q should satisfy the following condition: *q is the lowest denominator of the rational point* $x_m = \frac{p}{q}, x_m \in [x', x]$. As one sees, the value $L^*(y)$ governs the amplitude of the potential, while q controls the maximal 'resolution' and, hence, the total number of barriers.

3.2. Speculations about the continuous number of Cayley tree generations L and replica $n \to 0$ limit

Despite the many advantages of the RSB scheme, it contains the unavoidable in the replica formalism mystery of the $n \to 0$ limit, where $n = 2^L$ is the number of replicas (see figure 13).

One of the merits of our construction based on the Dedekind η-function consists in the possibility of changing continuously the number of ultrametric barriers and their heights by varying the parameter y, and hence changing continuously the number of states n of the RSB matrix. Let us recall that the standard 3-branching Cayley tree being isometrically embedded in the space $\mathcal{H} = \{z|\mathrm{Im}\, z > 0\}$ becomes a 'continuous' structure: one can define the smoothed neighbourhood of maxima of the function $f(z)$ in the half-plane $y = \mathrm{Im}\, z > 0$ (see figure 2). For instance, our construction allows us to increase continuously the number of states n from, say, $n = 1$ to $n = 2$ changing correspondingly the parameter y in the interval $[y_{n=1}, y_{n=2}]$, where $y_{n=1} = \frac{\sqrt{3}}{6}$ and $y_{n=2} = \frac{\sqrt{3}}{14}$.

Our geometric construction based on the isometric embedding of the Cayley tree into the complex plane permits us to consider also the opposite limit—the case when n is formally less than 1. This case means the absence of any states in the RSB matrix ($n = 0$). As one sees from figures 2 and 3, the function $f(z)$ no longer has local maxima above the value $y \equiv \mathrm{Im}\, z > \frac{\sqrt{3}}{2}$. As soon as we have identified the local maxima of the function $f(z)$ with the vertices (states) of the Cayley tree, we conclude that the absence of any states of the RSB matrix means the absence of local maxima of the function $f(z)$. Thus, the limit $n \to 0$ we interpret as $y \to \infty$. This claim is based on the behaviour of the function $f(z)$ in the upper

half-plane. The correspondence of the limits $n \to 0$ and $y \to \infty$ is schematically illustrated in figure 13.

The geometrical interpretation of the number of replica states in the region $0 < n < 1$ makes the physical statement about the 'analytic continuation $n \to 0$' more formal. Actually, let us recall the definition of the hyperbolic distance $\mathcal{L}$ in $\mathcal{H}(z|\mathrm{Im}\, z > 0)$ between two points $z_0 = (x_0, y_0)$ and $z = (x, y)$:

$$\cosh \mathcal{L} = 1 + \frac{(x - x_0)^2 + (y - y_0)^2}{y_0 y}. \tag{36}$$

As we have seen, the hyperbolic distance $\mathcal{L}$ is the continuous analogue of the number of Cayley tree generations, L, which permits us to define the number of replica states n as

$$n = \mathrm{e}^{\mathrm{const}\mathcal{L}}. \tag{37}$$

As $y \to 0$, we can replace $\cosh \mathcal{L}$ with the leading exponential term. This way we arrive at the standard relation $\mathrm{e}^{\mathcal{L}} = \frac{2y}{y_0}$. Hence,

$$\frac{\mathrm{e}^{\mathcal{L}}}{2} + \cancel{\frac{\mathrm{e}^{-\mathcal{L}}}{2}} = \frac{(x - x_0)^2 + y_0^2}{y_0 y} \tag{38}$$

neglecting the second term in the left-hand side of (38), we get

$$\mathcal{L} = -\ln y + c_1 \qquad (y \to 0)$$

where $c_1 = \ln \frac{2((x-x_0)^2+y_0^2)}{y_0}$. However if $y \to \infty$, equation (36) gives

$$\cancel{\frac{\mathrm{e}^{\mathcal{L}}}{2}} + \frac{\mathrm{e}^{-\mathcal{L}}}{2} = \frac{y}{y_0} \tag{39}$$

where according to the physical condition $n \to 0$ and equation (37), we have to take another branch of the function $\mathrm{arccosh}(\cdots)$, corresponding to the negative values of $\mathcal{L}$. This leads to the following definition of $\mathcal{L}$:

$$\mathcal{L} = -\ln y + c_2 \qquad (y \to \infty) \tag{40}$$

where $c_2 = \ln \frac{y_0}{2}$. As $y \to \infty$, the hyperbolic distance $\mathcal{L}$, defined according to (40), tends to $-\infty$. Equation (40) is consistent with the definition (37) of the number of replicas n in the region $0 < n < 1$. It would be very desirable to check how our conjecture works in the models possessing the RSB symmetry of the order parameter. We expect that our construction may be useful for the investigation of ageing phenomena considered from the point of view of the diffusion in the whole ultrametric space $\mathcal{H}(z|\mathrm{Im}\, z > 0)$.

Acknowledgments

The main part of this work has been accomplished owing to the hospitality of the laboratory LIFR-MIIP (CNRS, France and Independent University, Moscow); OV thanks the laboratory LPTMS (Université Paris Sud, Orsay) for the hearty welcome.

References

[1] Rammal R, Toulouse G and Virasoro M A 1986 *Rev. Mod. Phys.* **58** 765
[2] Brekke L and Freund P G O 1993 *Phys. Rep.* **233** 1
[3] Vladimirov V S, Volovich I V and Zelenov E I 1994 *p-Adic Analysis and Mathematical Physics* (Singapore: World Scientific)
[4] Mezard M, Parisi G and Virasoro M 1987 *Spin Glass Theory and Beyond* (Singapore: World Scientific)

[5] Parisi G 1979 *Phys. Rev. Lett.* **43** 1754
Parisi G 1980 *J. Phys. A: Math. Gen.* **13** L115
Parisi G 1980 *J. Phys. A: Math. Gen.* **13** 1101
Parisi G 1980 *J. Phys. A: Math. Gen.* **13** 1887
[6] Avetisov V A, Bikulov A V and Kozyrev S V 1999 *J. Phys. A: Math. Gen.* **32** 8785
[7] Parisi G and Sourlas N 2000 *Eur. Phys. J.* **14** 535
[8] Avetisov V A, Bikulov A V, Kozyrev S V and Osipov V A 2002 *J. Phys. A: Math. Gen.* **35** 177
[9] Avetisov V A, Bikulov A K and Osipov V A 2003 *J. Phys. A: Math. Gen.* **36** 4239
[10] Carlucci D M and De Dominicis C 1997 *C. R. Acad. Sci., Paris Mech. Phys. Chem. Astr.* **325** 527
[11] De Dominicis C, Carlucci D M and Temesvari T 1997 *J. Physique* I **7** 105
[12] Terras A 1985 *Harmonic Analysis on Symmetric Spaces and Applications I* (New York: Springer)
[13] Chandrassekharan K 1985 *Elliptic Functions* (Berlin: Springer)
[14] Di Francesco P, Senechal D and Mathieu P 1996 *Conformal Field Theory* (Berlin: Springer)
[15] Ogielski A T and Stein D L 1985 *Phys. Rev. Lett.* **55** 1634
[16] Bachas C P and Huberman B A 1987 *J. Phys. A: Math. Gen.* **20** 4995
[17] Magnus W 1974 *Noneuclidean Tesselations and Their Groups* (London: Academic)
[18] Beardon A F 1983 *The Geometry of Discrete Groups* (Berlin: Springer)